Electronic structure of $SrPt_4Ge_{12}$: Combined photoelectron spectroscopy and band structure study

H. Rosner,[1] J. Gegner,[2] D. Regesch,[2] W. Schnelle,[1] R. Gumeniuk,[1] A. Leithe-Jasper,[1] H. Fujiwara,[2] T. Haupricht,[2] T. C. Koethe,[2] H.-H. Hsieh,[3] H.-J. Lin,[4] C. T. Chen,[4] A. Ormeci,[1] Yu. Grin,[1] and L. H. Tjeng[2]

[1]*Max-Planck-Institut für Chemische Physik fester Stoffe, Nöthnitzer Straße 40, 01187 Dresden, Germany*

[2]*II. Physikalisches Institut, Universität zu Köln, Zülpicher Straße 77, 50937 Köln, Germany*

[3]*Chung Cheng Institute of Technology, National Defense University, Taoyuan 335, Taiwan*

[4]*National Synchrotron Radiation Research Center (NSRRC), 101 Hsin-Ann Road, Hsinchu 30077, Taiwan*

(Received 12 May 2009; published 14 August 2009)

We present a combined study of the electronic structure of the superconducting skutterudite derivative $SrPt_4Ge_{12}$ by means of x-ray photoelectron spectroscopy and full-potential band structure calculations including an analysis of the chemical bonding. We establish that the states at the Fermi level originate predominantly from the Ge 4*p* electrons and that the Pt 5*d* shell is effectively full. We find excellent agreement between the measured and the calculated valence-band spectra, thereby validating that band structure calculations in combination with photoelectron spectroscopy can provide a solid basis for the modeling of superconductivity in the compound series MPt_4Ge_{12} (M=Sr,Ba,La,Pr).

DOI: 10.1103/PhysRevB.80.075114 PACS number(s): 71.20.Eh, 79.60.−i

I. INTRODUCTION

Compounds with crystal structures featuring a rigid covalently bonded framework enclosing differently bonded guest atoms attracted much attention in the last decade. In particular, the skutterudite and clathrate families have been investigated in depth, and a fascinating diversity of physical phenomena is observed; many of which are due to subtle host-guest interactions. Among the skutterudites, the phenomena range from magnetic ordering to heavy-fermion and non-Fermi liquids, superconductivity, itinerant ferromagnetism, half metallicity, and good thermoelectric properties.[1–4] Superconductivity of conventional[5–7] and heavy-fermion type is found in skutterudites with T_c up to 17 K.[8–10]

The formula of the ternary filled skutterudites, being derived from the mineral $CoAs_3$, is given by $M_yT_4X_{12}$, with M as a cation, T as a transition metal, and X as usually a pnicogen (P, As, or Sb).[11] The M atoms reside in large icosahedral cages formed by $[TX_6]$ octahedra. A new family of superconducting skutterudites MPt_4Ge_{12} (M=Sr,Ba,La,Pr,Th) has been reported recently.[12–14] With trivalent La and Pr, T_c up to 8.3 K are observed. The compounds with the divalent cations Sr and Ba have lower T_c around 5.0 K.[12,13]

Band structure calculations predict that the electronic density of states (DOS) close to the Fermi level E_F is determined by Ge 4*p* states in all MPt_4Ge_{12} materials.[12,13,15] The position of E_F is adjusted by the electron count on the polyanionic host structure. This leads to the situation that the band structure at E_F can be shifted in an almost rigid-band manner by "doping" of the polyanion, which can be achieved either by charge transfer from the guest M or by the internal substitution of the transition metal T. Recently, this principle was demonstrated on the Pt-by-Au substitution in $BaPt_{4-x}Au_xGe_{12}$: while $BaPt_4Ge_{12}$ has a calculated DOS of 8.8 states/(eV f.u.), at the composition $BaPt_3AuGe_{12}$ the DOS is enhanced to 11.5 states/(eV f.u.).[16] Experimentally, an increase in the superconducting T_c from 5.0 to 7.0 K (Ref. 16) was observed. The rigid-band shift of the DOS peak at E_F with gold substitution is due to the Pt(Au) 5*d* electrons which, according to band structure calculations, lie rather deep below E_F and provide only a minor contribution to the DOS at E_F.[16]

Another prediction from the band structure calculations concerns the special role played by the Pt 5*d* states in $BaPt_4Ge_{12}$ ($SrPt_4Ge_{12}$) for the chemical bonding. It is known, assuming two-center-two-electron bonds within the *T*-*X* framework for the binary skutterudites that 72 electrons are required for the stabilization of the $[T_4X_{12}]$ formula unit.[1] In the case of $SrPt_4Ge_{12}$, the total number of *s* and *p* electrons of Sr, Pt, and Ge is $2+4\times2+12\times4=58$. To achieve the target value of 72, each Pt atom should use 3.5*d* electrons for bonding, which would be a rather large value compared to the one *d* electron per Co atom in Co_4As_{12} ($4\times CoAs_3$).

In order to determine the electron counts for $SrPt_4Ge_{12}$ as a characteristic for the chemical bonding, we evaluated the so-called electron localizability indicator (ELI)[17]. The combined analysis of the ELI and electron density (ED) (see Fig. 1) shows indeed three types of attractors in the valence region: two representing Ge-Ge bonds and one reflecting the Pt-Ge bond. No attractors were found between Sr and the framework atoms, suggesting predominantly ionic interaction here. The Ge-Ge bonds are two-electron bonds (electron counts 1.90 and 2.01), the Pt-Ge bond has a count of only 1.53 electrons, summing up to 60.18 electrons total per $[Pt_4Ge_{12}]$ formula unit. This means that only about 0.5 *d* electrons per Pt are participating in the stabilization of the $[Pt_4Ge_{12}]$ polyanion. Both procedures, valence electron counting and combined ELI/ED analysis, yield unusual results and raise the question about the role of 5*d* electrons of Pt in the formation of the MPt_4Ge_{12} compounds.

Up to now, no spectroscopic data are available to challenge the above-mentioned band structure predictions and chemical bonding analysis. Such a validation is important since one would like to know whether band theory can provide a solid basis for the modeling of superconductivity in

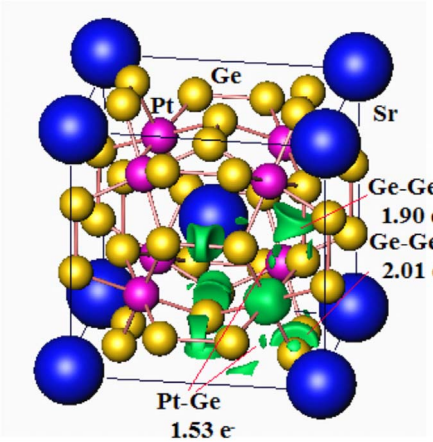

FIG. 1. (Color online) Chemical bonding in $SrPt_4Ge_{12}$: isosurface of ELI revealing Ge-Ge and Pt-Ge bonds together with their electron counts.

the MPt_4Ge_{12} (M=Sr,Ba,La,Pr) series. We therefore set out to perform a comparative study of the valence-band electronic structure of the superconducting skutterudite derivative $SrPt_4Ge_{12}$ by means of x-ray photoelectron spectroscopy (PES) and full-potential band structure calculations.

II. METHODS

Samples were prepared by standard techniques as described in Refs. 13 and 16. Metallographic and electron microprobe tests of polished specimens detected only traces of $PtGe_2$ (<4 vol %) and $SrPt_2Ge_2$ (<1 vol %) as impurity phases in the sample $SrPt_4Ge_{12}$. Electron probe micro analysis (EPMA) confirmed the ideal composition of the target phase. The lattice parameter is 8.6509(5) Å, as reported earlier.[13] For the cation position full occupancy was derived from full-profile crystal structure refinements of powder x-ray diffraction data, which are in good agreement with single-crystal data obtained in Ref. 12.

The PES experiments were performed at the Dragon beamline of the NSRRC in Taiwan using an ultrahigh-vacuum system (pressure in the low 10^{-10} mbar range) which is equipped with a Scienta SES-100 electron energy analyzer. The photon energy was set to 700 and 190 eV. The latter energy is close to the Cooper minimum in the photoionization cross section of the Pt 5d valence shell.[18] The overall energy resolution was set to 0.35 eV and 0.25 eV, respectively, as determined from the Fermi cutoff in the valence band of a Au reference which was also taken as the zero of the binding-energy scale. The $4f_{7/2}$ core level of Pt metal was used as an energy reference too. The reference samples were scraped *in situ* with a diamond file. The polycrystalline $SrPt_4Ge_{12}$ sample with dimensions of $2\times2\times3$ mm^3 was cleaved *in situ* exposing a shiny surface and measured at room temperature at normal emission.

Electronic structure calculations within the local-density approximation (LDA) of the density functional theory were employed using the full-potential local-orbital code FPLO (version 5.00–19).[19] In the full-relativistic calculations, the exchange and correlation potential of Perdew and Wang[20] was used. As the basis set, Sr(4s,4p,5s,5p,4d), Pt(5s,5p,6s,6p,5d), and Ge(3d,4s,4p,4d) states were employed. Lower-lying states were treated as core. A very dense k mesh of 1256 points in the irreducible part of the Brillouin zone ($30\times30\times30$ in the full zone) was used to ensure accurate DOS information.

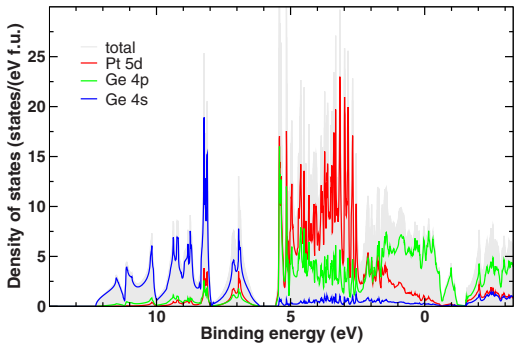

FIG. 2. (Color online) Calculated total and atom resolved partial electronic density of states of $SrPt_4Ge_{12}$. The Fermi level is at zero energy.

The electron localizability indicator was evaluated according to Ref. 17 with an ELI/ELF module implemented within the FPLO program package.[21] The topology of ELI was analyzed using the program BASIN (Ref. 22) with subsequent integration of the electron density in basins, which are bound by zero-flux surfaces in the ELI gradient field. This procedure, similar to the one proposed by Bader for the electron density,[23] allows to assign an electron count for each basin, providing fingerprints of direct (covalent) interactions.

III. RESULTS AND DISCUSSION

Figure 2 shows the calculated DOS for $SrPt_4Ge_{12}$ (E_F is at zero binding energy). The valence band is almost exclusively formed by Pt and Ge states. The low and featureless Sr DOS indicates that it plays basically the role of a charge reservoir. Further inspection of the DOS shows that the high-lying states between about 6 and 12 eV binding energies originate predominantly from Ge 4s electrons, whereas the lower-lying part of the valence band is formed by Pt 5d and Ge 4p states. The Pt 5d states essentially form a narrow band complex of approximately 3 eV bandwidth centered at about 4 eV binding energy. Our calculated DOS is in good agreement with the previous results of Bauer *et al.*[12]

Figure 3 displays the valence-band photoemission spectra of $SrPt_4Ge_{12}$ taken with a photon energy of $h\nu$=700 eV (upper panel) and 190 eV (middle panel), together with the reference spectrum of elemental Pt metal (bottom panel). The spectra are normalized to their integrated intensities after an integral background has been subtracted to account for inelastic scattering. All spectra show a clear cutoff at E_F (zero binding energy) consistent with the systems being good metals. It is of no surprise that the 700 eV spectrum of $SrPt_4Ge_{12}$ is very different from that of Pt since they are different materials. More interesting is that there are also differences between the 700 and 190 eV spectra of $SrPt_4Ge_{12}$ itself. This is

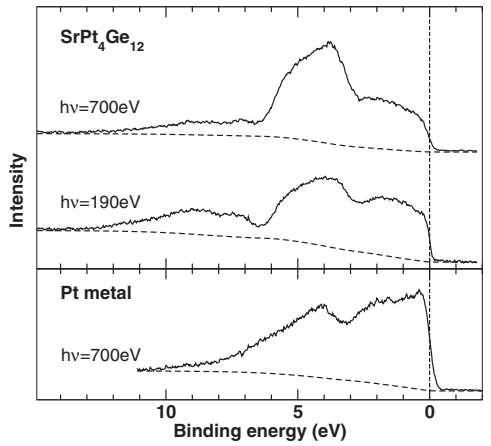

FIG. 3. Valence-band photoemission spectra of $SrPt_4Ge_{12}$ taken with a photon energy of $h\nu$=700 eV (upper panel) and 190 eV (middle panel). As reference, the valence-band spectrum of elemental Pt metal taken at $h\nu$=700 eV is also given (bottom panel). The spectra are normalized with respect to their integrated intensities after subtracting an integral background indicated by the dashed curves.

caused by differences in the photon energy dependence of the photoionization cross section of the relevant subshells forming the valence band, in this case, the Ge 4*s*, 4*p*, and Pt 5*d*.[18] In fact, we chose those 190 and 700 eV photon energies in order to make optimal use of the cross-section effects for identifying the individual contributions of the Ge and Pt states to the valence band as we will show in the next sections. In particular, at 700 eV, the Pt 5*d* cross section is calculated to be a factor of 3.9 larger than that of the Ge 4p, while at 190 eV (close to the Cooper minimum for the Pt 5*d*) it is equal or even slightly smaller, i.e., a factor of 0.92 (see Table I). In other words, the 700 eV spectra are dominated by the Pt 5*d* contribution, while at 190 eV the contributions become comparable.

The intensity I of a normalized spectrum as depicted in Fig. 3 is built up from the Pt 5*d*, Ge 4*p*, and Ge 4*s* partial DOS (ρ) weighted with their respective photoionization cross sections (σ). This is formulated in Eqs. (1) and (2) which take into account that the cross sections at 190 eV photon energy are different from those at 700 eV, respectively. The proportionality factors c_{190} and c_{700}, respectively, also enter here since the absolute values for the photon flux and the transmission efficiency of the electron energy analyzer are not known. In addition, the constants α, β, and γ are introduced to express the nonuniqueness in the calculation of the weight of the Pt 5*d*, Ge 4*p*, and Ge 4*s* DOS, respectively, since these depend (somewhat) on which calculational method has been used,

$$I_{190} = c_{190}[\sigma_{190}^{\text{Pt }5d}\alpha\rho^{\text{Pt }5d} + \sigma_{190}^{\text{Ge }4p}\beta\rho^{\text{Ge }4p} + \sigma_{190}^{\text{Ge }4s}\gamma\rho^{\text{Ge }4s}], \tag{1}$$

$$I_{700} = c_{700}[\sigma_{700}^{\text{Pt }5d}\alpha\rho^{\text{Pt }5d} + \sigma_{700}^{\text{Ge }4p}\beta\rho^{\text{Ge }4p} + \sigma_{700}^{\text{Ge }4s}\gamma\rho^{\text{Ge }4s}]. \tag{2}$$

Using the predictions of the band structure calculations as a guide, we notice that the Ge 4*s* states hardly give a contribution in the energy range between the Fermi level and 6 eV binding energy. In this range, i.e., most relevant for the properties, the valence band seems to be determined mostly by the Pt 5*d* and Ge 4*p* states. We now analyze the experimental spectra along these lines. Using Eqs. (1) and (2), the Pt 5*d* and Ge 4*p* DOS can be experimentally extracted as follows:

$$\rho^{\text{Pt }5d} \sim I_{700} - A \times I_{190}, \tag{3}$$

$$\rho^{\text{Ge }4p} \sim I_{190} - B \times I_{700}, \tag{4}$$

with the parameters $A=(c_{700}/c_{190})(\sigma_{700}^{\text{Ge }4p}/\sigma_{190}^{\text{Ge }4p})$ and $B=(c_{190}/c_{700})(\sigma_{190}^{\text{Pt }5d}/\sigma_{700}^{\text{Pt }5d})$. While the cross sections σ can be readily obtained from Table I, it would be an enormous task to determine (experimentally) the ratio between c_{700} and c_{190}. Thus, since it is difficult to obtain directly an estimate for A and B, we use the product AB given by $(\sigma_{190}^{\text{Pt }5d}/\sigma_{190}^{\text{Ge }4p})/(\sigma_{700}^{\text{Pt }5d}/\sigma_{700}^{\text{Ge }4p})$, which can be calculated from Table I to be about 0.92/3.9=0.24. Therefore, we vary the values for A and B under the constraint that AB=0.24, searching for difference spectra which reproduce both the Pt 5*d* and the Ge 4*p* DOS as obtained by the band structure calculations.

We find good results for A=0.6 and B=0.4 as displayed in Figs. 4 and 5. Focusing first at Fig. 4 in which the rescaled 190 eV spectrum is subtracted from the 700 eV one, we can observe that the difference spectrum resembles very much that of the calculated Pt 5*d* DOS. Here, the latter has been broadened to account for the experimental resolution and lifetime effects. Interestingly, the main Pt intensity is positioned at around 3–6 eV binding energies and its weight near the E_F region is very small. The experiment fully confirms this particular aspect of the theoretical prediction, which is important for the modeling of the superconducting properties as discussed above. We would like to note that the main peak of the calculated Pt 5*d* DOS is positioned at a somewhat lower binding energy than that of the experimental difference spectrum. Similar small deviations have been observed in other intermetallic materials[24,25] and can be attributed to the inherent limitations of mean-field methods, such as the LDA, to calculate the dynamic response of a system.

TABLE I. Calculated photoionization cross sections per electron (σ in Mb/e) for the Pt 5*d*, Ge 4*p* and Ge 4*s* subshells, from Yeh and Lindau (Ref. 18).

$h\nu$ (eV)	$\sigma^{\text{Pt }5d}$	$\sigma^{\text{Ge }4p}$	$\sigma^{\text{Ge }4s}$	$\sigma^{\text{Pt }5d}/\sigma^{\text{Ge }4p}$	$\sigma^{\text{Pt }5d}/\sigma^{\text{Ge }4s}$
190	0.0099	0.0108	0.021	0.92	0.47
700	0.0074	0.0019	0.0030	3.9	2.5

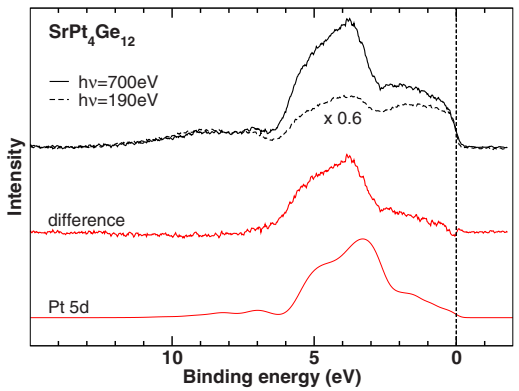

FIG. 4. (Color online) Normalized and background-corrected valence-band photoemission spectra of $SrPt_4Ge_{12}$ taken with a photon energy of $h\nu$=700 eV (black solid line) and 190 eV (black dashed line). The 190 eV spectrum has been rescaled with a factor of 0.6 (see text). The difference spectrum (red solid line) is compared to the calculated Pt 5*d* DOS (red thin line).

Figure 5 shows the difference of the spectrum taken at 190 eV and the rescaled spectrum at 700 eV. This experimental difference spectrum reveals structures which can be divided into two major energy regions: the first region extends from 0 to 6 eV binding energy and the second from 6 to 12 eV. For the first region, we can make a comparison with the calculated Ge 4*p* DOS since the calculated Ge 4*s* contribution is negligible as explained above. We obtain a very satisfying agreement between the experiment and theory for the Ge 4*p* states. In particular, we would like to point out that the experiment confirms the strong presence the Ge 4*p* states in the vicinity of the Fermi level E_F. Looking now at the second region (between 6 and 12 eV), we see that the calculated Ge 4*s* DOS also reproduces nicely the shape and the energy position of the experimental difference spectrum. Since the scaling parameters *A* and *B* for the intensity of the spectra have been determined between 0 and 6 eV binding energy, where the contribution of Ge 4*s* states is small, a better

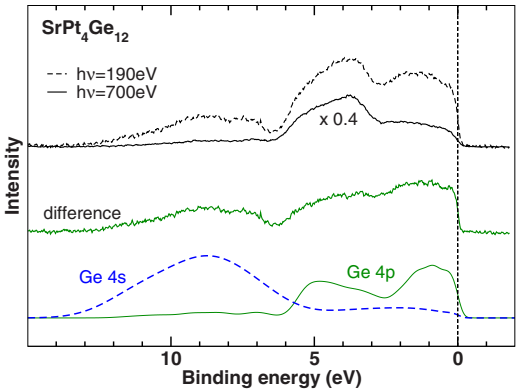

FIG. 5. (Color online) Normalized and background-corrected valence-band photoemission spectra of $SrPt_4Ge_{12}$ taken with a photon energy of $h\nu$=190 eV (black dashed line) and 700 eV (black-solid line). The 700 eV spectrum has been rescaled with a factor of 0.4. The difference spectrum (green solid line) is compared to the calculated Ge 4*p* DOS (green thin line) and Ge 4*s* DOS (blue dashed line).

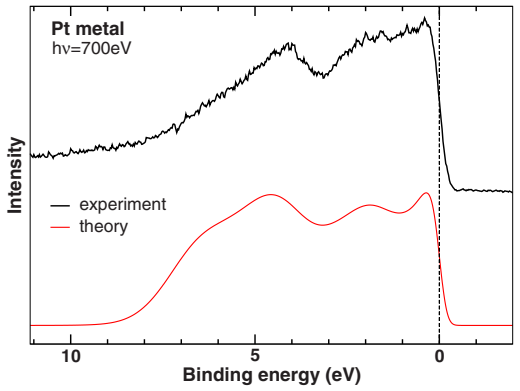

FIG. 6. (Color online) Valence-band photoemission spectrum of elemental Pt metal taken with a photon energy of $h\nu$=700 eV (black-solid line) and the calculated Pt 5*d* DOS (red-solid line).

agreement of the Ge 4*s* related intensity between 6 and 12 eV binding energy cannot be expected. Here, we remark that the calculated Ge 4*p* DOS has a negligible contribution in this region.

As a further check, we also perform a comparison between the experimental photoemission spectrum of elemental Pt metal and the corresponding calculated Pt 5*d* DOS. The result is shown in Fig. 6. Also, here we find satisfying agreement between experiment and theory. The Pt 5*d* states range from 9 eV binding energy all the way up to E_F. Clearly, the high Fermi cutoff in Pt metal is formed by these Pt 5*d* states, in strong contrast to the $SrPt_4Ge_{12}$ case.

Figure 7 shows the Pt 4*f* core levels of $SrPt_4Ge_{12}$ (top) and elemental Pt metal (bottom). The spectra exhibit the characteristic spin-orbit splitting giving the $4f_{5/2}$ and $4f_{7/2}$ peaks. For $SrPt_4Ge_{12}$, the peak positions for the $4f_{5/2}$ and $4f_{7/2}$ are 75.4 and 72.1 eV binding energy, respectively. For Pt metal, the values are 74.4 and 71.1 eV, respectively. The spin-orbit splitting is thus 3.3 eV for both materials. This compares well with the calculated spin-orbit splitting of about 3.45 eV for both compounds from the LDA calculations.

Remarkable is that the $SrPt_4Ge_{12}$ 4*f* peaks are shifted by 1 eV to higher binding energies in comparison to those of Pt

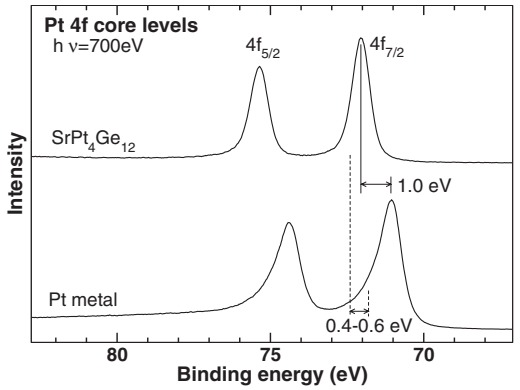

FIG. 7. Pt 4*f* core-level photoemission spectra of $SrPt_4Ge_{12}$ (top) and elemental Pt metal (bottom). Solid vertical lines represent the peak positions of the $4f_{7/2}$ levels; dashed vertical lines represent the center of gravity positions (see text).

metal. Similar shifts have also been observed in other noble-metal intermetallic compounds,[24–26] indicating a more dilute electron density around the noble-metal sites. To compare this chemical shift to LDA calculations, one has to take into account that the LDA does not incorporate many-body effects of the final state, manifesting in the asymmetric line shape of the spectra as discussed below in more detail. But it can be shown[27] that final-state effects do not alter the average energy of the spectrum. If we determine the center of gravity of the $4f_{7/2}$, we find a binding energy of 72.4 eV for $SrPt_4Ge_{12}$ and 71.9 ± 0.2 eV (indicated by dashed lines in Fig. 7) for Pt metal, resulting in a chemical shift of 0.4 to 0.6 eV. This agrees well with the shift obtained from our band structure calculations which amounts to 0.43 eV.

One can clearly observe that the line shape of the core levels in $SrPt_4Ge_{12}$ is narrower and not as asymmetric as in the case of Pt metal. An asymmetry in the line shape is caused by the presence of electron-hole pair excitations upon the creation of the core hole, i.e., screening of the core hole by conduction-band electrons, and can be well understood in terms of the Doniac-Sunjic theory.[28] The strong asymmetry of the $4f$ of Pt metal can therefore be taken as an indication for the high DOS with Pt $5d$ character at E_F.[29] The rather symmetric line shape of the $4f$ of $SrPt_4Ge_{12}$, on the other hand, indicates very low DOS at E_F. All this confirms the results of the valence-band measurements: the main intensity of the Pt $5d$ band is at 3–6 eV binding energies, strongly reducing its weight at E_F.

IV. CONCLUSION

In conclusion, we find excellent agreement between the measured photoemission spectra and the LDA band structure calculations for $SrPt_4Ge_{12}$. This provides strong evidence that correlation effects beyond the LDA are of minor relevance in this compound. The excellent agreement confirms the picture of the chemical bonding analysis yielding rather deep lying Pt $5d$ states which only partially form covalent bands with the Ge $4p$ electrons. In turn, the states at the Fermi level that are relevant for the superconducting behavior of this compound can be firmly assigned to originate predominantly from Ge $4p$ electrons. This study provides strong support that the band theory is a good starting point for the understanding of the electronic structure of the MPt_4Ge_{12} (M=Sr, Ba, La, Pr, Th) material class and is thus of valuable help in the search for new compositions with higher superconducting transition temperatures.

[1] C. Uher, Semicond. Semimetals **68**, 139 (2001).
[2] B. C. Sales, *Handbook on the Physics and Chemistry of Rare Earths* (Elsevier, Amsterdam, 2003), Vol. 33, Chap. 211, pp. 1–34.
[3] A. Leithe-Jasper, W. Schnelle, H. Rosner, N. Senthilkumaran, A. Rabis, M. Baenitz, A. Gippius, E. Morozova, J. A. Mydosh, and Yu. Grin, Phys. Rev. Lett. **91**, 037208 (2003); **93**, 089904(E) (2004).
[4] G. S. Nolas, D. T. Morelli, and T. Tritt, Annu. Rev. Mater. Sci. **29**, 89 (1999).
[5] G. Meisner, Physica B & C **108**, 763 (1981).
[6] H. Kawaji, H.-o. Horie, S. Yamanaka, and M. Ishikawa, Phys. Rev. Lett. **74**, 1427 (1995).
[7] K. Tanigaki, T. Shimizu, K. M. Itoh, J. Teraoka, Y. Moritomo, and S. Yamanaka, Nature Mater. **2**, 653 (2003).
[8] E. D. Bauer, N. A. Frederick, P.-C. Ho, V. S. Zapf, and M. B. Maple, Phys. Rev. B **65**, 100506(R) (2002).
[9] M. Imai, M. Akaishi, E. H. Sadki, T. Aoyagi, T. Kimura, and I. Shirotani, Phys. Rev. B **75**, 184535 (2007).
[10] I. Shirotani, S. Sato, C. Sekine, K. Takeda, I. Inagawa, and T. Yagi, J. Phys.: Condens. Matter **17**, 7353 (2005).
[11] The parameter y in $M_yT_4X_{12}$ ($y \leq 1$) indicates the (likely intrinsic) incomplete filling of the M site for several compounds in the family.
[12] E. Bauer *et al.*, Phys. Rev. Lett. **99**, 217001 (2007).
[13] R. Gumeniuk, W. Schnelle, H. Rosner, M. Nicklas, A. Leithe-Jasper, and Yu. Grin, Phys. Rev. Lett. **100**, 017002 (2008).
[14] D. Kaczorowski and V. H. Tran, Phys. Rev. B **77**, 180504(R) (2008).
[15] V. H. Tran, D. Kaczorowski, W. Miiller, and A. Jezierski, Phys. Rev. B **79**, 054520 (2009).
[16] R. Gumeniuk, H. Rosner, W. Schnelle, M. Nicklas, A. Leithe-Jasper, and Yu. Grin, Phys. Rev. B **78**, 052504 (2008).
[17] M. Kohout, Int. J. Quantum Chem. **97**, 651 (2004).
[18] J. J. Yeh and I. Lindau, At. Data Nucl. Data Tables **32**, 1 (1985).
[19] K. Koepernik and H. Eschrig, Phys. Rev. B **59**, 1743 (1999).
[20] J. P. Perdew and Y. Wang, Phys. Rev. B **45**, 13244 (1992).
[21] A. Ormeci, H. Rosner, F. R. Wagner, M. Kohout, and Yu. Grin, J. Phys. Chem. A **110**, 1100 (2006).
[22] M. Kohout, BASIN, version 4.7 (2008).
[23] R. F. W. Bader, *Atoms in Molecules: A Quantum Theory* (Oxford University Press, New York, 1990).
[24] J. Gegner, T. C. Koethe, H. Wu, H. Hartmann, T. Lorenz, T. Fickenscher, R. Pöttgen, and L. H. Tjeng, Phys. Rev. B **74**, 073102 (2006).
[25] J. Gegner, H. Wu, K. Berggold, C. P. Sebastian, T. Harmening, R. Pöttgen, and L. H. Tjeng, Phys. Rev. B **77**, 035103 (2008).
[26] N. Franco, J. E. Klepeis, C. Bostedt, T. Van Buuren, C. Heske, O. Pankratov, T. A. Callcott, D. L. Ederer, and L. J. Terminello, Phys. Rev. B **68**, 045116 (2003).
[27] B. I. Lundqvis, Phys. Kondens. Mater. **9**, 236 (1969).
[28] S. Doniach and M. Sunjic, J. Phys. C **3**, 285 (1970).
[29] S. Hüfner and G. K. Wertheim, Phys. Rev. B **11**, 678 (1975).